Latin American Journal of Aquatic Research, 47(2): 270-281, 2019
DOI: 10.3856/vol47-issue2-fulltext-7

Research Article

New coral reef structures in a tropical coral reef system

Francisco Liaño-Carrera[1], Tomás Camarena-Luhrs[2], Arturo Gómez-Barrero[3]
Francisco Javier Martos-Fernández[4], José Isaac Ramírez-Macias[3] & David Salas-Monreal[4]
[1]Administracion Portuaria Integral de Veracruz, Veracruz, México
[2]Comision Nacional de Áreas Naturales Protegidas de Veracruz, Veracruz, México
[3]ARGO Consultores, Puebla, México
[4]Universidad Veracruzana, Xalapa, México
Corresponding author: David Salas-Monreal (davsalas@uv.mx)

ABSTRACT. A multibeam sonar combined with an Acoustic Doppler Current Profiler (ADCP) were used at the Veracruz Reef System (VRS), Gulf of Mexico, during the spawning period of August 2016 in order to elucidate plankton trajectories within the study area. The new high-resolution bathymetry provided the location of 50 coral reefs, 27 more reefs than known at the VRS. Most of those reefs are submerged reefs located at depths greater than 40 m. The total coral reef area of the VRS was calculated in 70.1557 km^2. Only ~10% of the total area corresponds to submerged reefs. Forty-eight species were identified, seven more than known species at the VRS, 45 of the order of Escleractinia and 3 of the order of Anthoathecatae. *Acropora prolifera*, a hybrid, was also identified in most reefs. All species were observed in the emerged and submerged reefs. The distance at which the three local river discharges (Jamapa, La Antigua, and Actopan) brought sediments to the VRS was calculated. Those are inappropriate areas for coral settlement or development due to sediment transport and temperature and salinity fluctuation. Finally, light penetration was measured at 19 m depth near one reef structure during August 2016 suggesting that even during cloud coverage and rain periods there was a light bioavailability at the sampling point.

Keywords: coral reef species; tropical reef systems; larvae dispersion; Veracruz Reef System; Gulf of Mexico

INTRODUCTION

The Veracruz Reef System (VRS), one of the most studied reef areas (Salas-Pérez & Granados-Barba, 2008) of the western Gulf of Mexico, is located off the coast of Veracruz, one of the oldest cities in America (1519). The hydrographic characteristics of the VRS (Salas-Pérez & Arenas-Fuentes, 2011) are the result of a mixing process generated by a combination of cold fronts; river discharges (Avendaño-Alvarez *et al.*, 2017) and the Loop Current and its collision with the continental slope (Monreal-Gómez *et al.*, 2004). This phenomenon has led to the idea of a direct connection between the coral reef systems of the Caribbean Sea with those of the western Gulf of Mexico (Villegas-Sánchez *et al.*, 2013). Thus, there is connectivity among those systems, sharing fish and coral species. A total of 23 coral reef areas were previously described in the VRS (DOF, 1992) and from those, only three have been described as coral larvae providers to the northern coral reef areas (Tuxpan-Lobos reef area) of the western Gulf of Mexico (Chacón-Gómez *et al.*, 2013). Due to the distance between the reef systems (~250 km), to current patterns and to the time of the plankton stage of some organisms, previous studies have suggested the presence of several reef structures between them (Salas-Monreal *et al.*, 2017). However, some of those submerged reef areas are only locally known.

At coastal scale, the distribution of the currents in the VRS has been attributed to the complex bathymetry and the presence of coral reefs and islands (Salas-Monreal *et al.*, 2009). These characteristics have led to the conclusion that the bathymetry and local winds modulate the circulation at the VRS. Around the reefs and islands the abrupt bathymetric changes generates cyclonic eddies (Riveron-Enzastiga *et al.*, 2016), those eddies are considered highly productive areas, owing to

Corresponding editor: Eduardo Quiroga

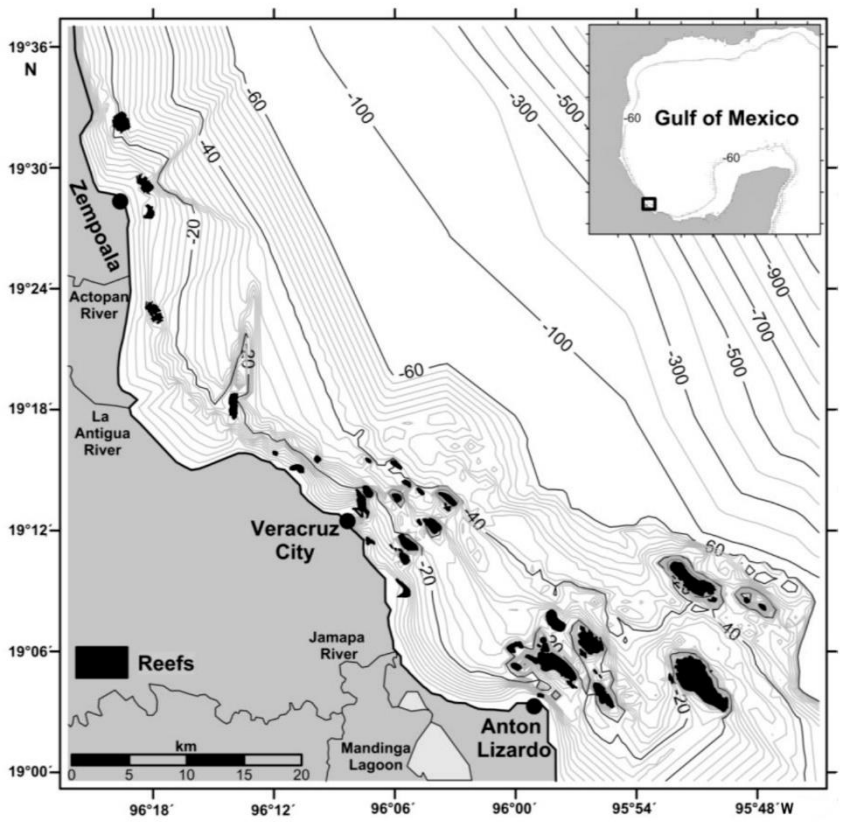

Figure 1. The Veracruz Reef System (VRS). Bathymetry (m) and the location of the coral reef structures.

high nutrient cold deep water (Salas-de-Leon *et al.*, 2004), while the anticyclonic eddies are considered oligotrophic (Biggs, 1992). Salas-Monreal *et al.* (2009) found a cyclonic eddy off the Jamapa River (Fig. 1) during the summer season. They attributed the eddy to current rectification owing to the presence of the Cape of Anton Lizardo (Fig. 1), this was assumed since no promontories or coral reef structures were reported in the area, further, it was assumed that the area located off the Jamapa River had a gentle slope toward the continental slope.

Based on current patterns, the VRS has several complex patterns due to its complex bathymetry, however, the two general patterns could be described as currents with a northward direction, during the spring and summer seasons, and currents with a predominant southward direction, during the autumn and winter seasons (Salas-Pérez *et al.*, 2012), bringing cold water to the system. The water temperature is an important parameter in the marine environment since it controls the rate at which biological processes and chemical reactions are carried out. It also determines the global distribution of marine species (Lalli & Parsons, 1997). In shallow areas, such as the VRS, the temperature variation depends on the season of the year (Avendaño-Alvarez *et al.*, 2017). During the rainy season, the Jamapa River discharges create sub-optimal conditions for the development of corals in the area (Horta-Puga *et al.*, 2015), with a well-developed thermocline at 5 m depth, with salinity values as low as 20 (Salas-Monreal *et al.*, 2009). Vidal *et al.* (1994) mention that the salinity distribution in the western Gulf of Mexico is determined by the location of the anticyclonic eddies, which varies depending on the season (Riveron-Enzastiga *et al.*, 2016). During the dry season, in contrast, the temperature could be as high as 34°C (Avendaño-Alvarez *et al.*, 2017) with salinity values of up to 38 owing to high evaporation spots (Salas-Monreal *et al.*, 2009). The salinity variation can affect the physiological functions of organisms by altering its osmotic balance, affecting their distribution and behavior (Mann & Lazier, 1991; Lalli & Parsons, 1997). At the local scale (~1 km), the temperature and salinity may also vary depending on the presence of cyclonic (low temperature and high salinity) and anticyclonic (low salinity and high temperature) eddies, generated by abrupt bathymetric changes, such as submerged reefs and promontories. In the VRS, eddies have previously been described with a general interpretation of their dynamics assuming a relatively flat bottom, owing to the absence of an accurate bathymetry of the area (*e.g.*, Salas-Monreal *et al.*, 2009; Riveron-Enzastiga *et al.*, 2016).

The VRS has abrupt bathymetric changes which generate eddies that modify the temperature and salinity, affecting the solubility of oxygen, which increases by decreasing the temperature and salinity (Alvarado & Aguilar, 2009). The oxygen on the western Gulf of Mexico is modulated by the Caribbean Sea, with an average concentration of 4 to 5 mL L^{-1} (De La Lanza Espino, 2001). These values may vary in areas with abrupt bathymetric changes due to the formation of eddies and the water column mixture generated by the rectification of the current in shallow areas (bottom friction) under the effect of the wind (surface friction). Avendaño-Alvares *et al.* (2017) found a hypoxic area off the Jamapa River due to bacterial activities and the presence of a cyclonic eddy. The oxygen is one of the most important gases since it is necessary for the survival of the majority of marine organisms. The lower levels may be indicative of high bacterial concentrations (Rogers *et al.*, 2001) while the higher levels may be indicative of high chlorophyll-*a* concentration.

The dispersion of plankton and ichthyoplankton is influenced by a wide range of biological and physical processes (Farrell *et al.*, 1991). Eddies and fronts, around the reefs, are of great importance to understand the local dynamics of coral and fish recruitment as well as the dispersal of organisms within the reefs (Chacón-Gómez *et al.*, 2013). Hamner & Haury (1981) describe the formation of eddies around reefs. The surface water during high tide periods reaches above the reef, making the flow to fall head-on creating a physical barrier around the reef, which also forms stationary swirls on the reef crest. On the other hand, fronts can be generated in coastal areas where tidal currents interact with the topography. Fronts are formed due to the transition between two water masses of different salinity and temperature; these areas have been correlated with high concentrations of chlorophyll-*a* (Bakun, 1996).

Therefore, this study aims to describe the coral larvae biovolume trajectories and concentration areas, during the spawning period of August 2016, using a new and accurate bathymetry of the area, in order to better understand local dynamics and coral larvae dispersion within the VRS. This information should also explain the reason for the absence of coral reef structures, in some coral larvae concentration areas.

MATERIALS AND METHODS

Current velocities, biovolumes, temperature, salinity, and light intensity time series were obtained at the Veracruz Reef System (VRS), during the coral spawning period of August 2016 (Fig. 1). One light data logger HOBO (UA-002-64 HOBO) was deployed near Isla Sacrificios reef (Table 1) from August 1st to 30th, in order to describe any change in light penetration during the spawning period of 2016. Light intensity was taken every 15 min at a depth of 19 m. Current velocity data were recorded continuously along the study area at a mean speed of ~5 m s^{-1} (Salas-Monreal *et al.*, 2009) on August 28th, 2016, 10 days after the full moon of August (18/08/2016). The 300-kHz vessel-mounted ADCP recorded one data every second uninterruptedly for four days. Current velocities were corrected in order to eliminate the current tidal velocity (Salas-Pérez *et al.*, 2012). The 1 Hz pin rate of the ADCP was averaged every 10 s, in order to obtain one data every ~50 m, with a blanking space of ~0.8 m at the surface and ~1 m near the bottom. A global positioning system (GPS) dataset coupled with the ADCP allows the exact location of the temperatures and currents at each second. The GPS was also used to correct the internal gyro compass of the ADCP following the method of Trump & Marmorino (1997). Finally, all data were interpolated using the triangulation with linear interpolation method (Salas-de-León *et al.*, 2004), this method provides a synoptic view of the studied area (Salas-Monreal *et al.*, 2009).

The 300-kHz ADCP was also used to describe larvae concentrations during the sampling period (Chacón-Gómez *et al.*, 2013), this was possible since the ADCP has an optimal response to scatters of about 5 mm (Zhu *et al.*, 2000). No biological recollection was performed during the sampling period in order to avoid any possible perturbation of the system; however, previous work has proved that zooplankton in the VRS is mainly composed by copepods (Lozano-Aburto, 2008). The backscatter intensity of the ADCP was then corrected to compute vertically integrated acoustic scattering volumes (Holliday & Pieper, 1980; Flagg & Smith, 1989; Storlazzi *et al.*, 2006; Salas-Monreal *et al.*, 2009) in order to obtain the contour maps of the biovolume as an approximation of zooplankton biovolumes with a size of ~5 mm. This information was visually corroborated (observing areas of high and low biovolumes, respectively).

Due to the absence of an accurate bathymetry of the SAV, a multibeam sonar was used to obtain the bathymetry of the area with a resolution of ~1 m; the first time that the bathymetry of a coral reef area was obtained with such precision in the Gulf of Mexico. It took more than six months to cover the entire area. The bathymetry was then corrected in order to avoid tidal variations (Salas-Monreal *et al.*, 2017), using the sea level height of the national tide gauge at Veracruz (Veracruz City, Fig. 1). Due to the new bathymetry, a total of 50 coral reef structures were located, 27 more than the 23 previously known (DOF, 1992). Finally, a

Table 1. Name, location and area of each coral reef of the Veracruz Reef System.

Reef name	Latitude (N)	Longitude (W)	Area (km^2)	Reef type
Amarillo	19°32´15"	96°19´35"	1.862	sumberged
Tia Juana	19°29´11"	96°18´24"	1.117	emerged
Juan Ángel	19°27´46"	96°18´10"	0.641	emerged
Rincon	19°22´50"	96°17´56"	1.231	emerged
Montenegro	19°18´12"	96°14´00"	1.408	sumberged
Punta Brava	19°15´50"	96°11´56"	0.111	emerged
Ahogado Punta Gorda	19°15´35"	96°09´51"	0.185	sumberged
Los Verdes	19°15´29"	96°07´19"	0.078	sumberged
Las Holandesas 1	19°15´14"	96°05´53"	0.125	sumberged
Punta Gorda	19°15´02"	96°10´43"	0.935	emerged
Las Holandesas 2	19°14´20"	96°05´23"	0.264	sumberged
Las Holandesas 3	19°13´55"	96°04´43"	0.106	sumberged
Galleguilla	19°13´52"	96°07´20"	0.800	emerged
La Blanquilla	19°13´36"	96°05´53"	1.056	emerged
Anehada de adentro	19°13´35"	96°03´20"	1.672	emerged
La Gallega	19°13´19"	96°07´36"	1.855	emerged
Ahogado de Guilligan	19°13´19"	96°02´28"	0.012	sumberged
Ahogado de Andrea	19°13´12"	96°03´27"	0.012	sumberged
Ahogado Chico	19°13´09"	96°03´17"	0.013	sumberged
Ahogado Grande	19°13´06"	96°03´20"	0.035	sumberged
Ahogado del Jurel	19°13´02"	96°03´25"	0.028	sumberged
Bajo Paduca	19°12´25"	96°04´46"	0.225	sumberged
Isla Verde	19°12´14"	96°04´04"	1.451	emerged
Hornos	19°11´26"	96°07´15"	0.546	emerged
Pajaros	19°11´19"	96°05´23"	1.470	emerged
Ahogado del Caracol	19°11´14"	96°06´11"	0.036	sumberged
Mersey	19°11´01"	96°05´44"	0.065	sumberged
Ahogado Terranova	19°11´00"	96°05´57"	0.017	sumberged
Isla Sacrificios	19°10´34"	96°05´33"	0.628	emerged
Anegada de Afuera	19°09´35"	95°51´27"	6.785	emerged
Ingeniero	19°09´01"	96°05´26"	1.311	emerged
Santiaguillo	19°08´34"	95°48´31"	0.880	emerged
Bajo Enmedio	19°08´31"	95°50´21"	0.039	sumberged
Topatillo	19°08´30"	95°50´08"	0.264	emerged
Anegadilla	19°08´14"	95°47´42"	1.004	emerged
La Palma	19°07´26"	95°58´03"	1.994	sumberged
Enmedio	19°06´25"	95°56´18"	5.390	emerged
Blanca	19°06´19"	96°00´08"	0.652	emerged
Ahogado medio	19°06´16"	95°58´51"	0.047	sumberged
Polo	19°06´12"	95°58´29"	0.174	emerged
Sargazo	19°05´45"	95°56´33"	0.304	sumberged
Chopas	19°05´21"	95°58´05"	10.314	emerged
Giote	19°05´16"	96°06´00"	0.976	emerged
Ahogado Cabezo	19°05´01"	95°50´17"	0.011	sumberged
Periferico	19°04´59"	95°56´02"	0.046	sumberged
Ahogado de Rizo	19°04´46"	95°55´48"	0.026	sumberged
Ahogado del Pez León	19°04´37"	95°52´16"	0.207	sumberged
Cabezo	19°04´33"	95°50´55"	15.387	emerged
Rizo	19°04´06"	95°55´49"	6.162	emerged
Punta Coyol	19°03´46"	95°58´47"	0.202	sumberged

visual inspection of the coral reefs leads to the description of 48 species in the area, done using at least eight linear transects at each reef site. Most of the previously unknown reefs are located at greater depths than 30 m. Perhaps this is one of the reasons to be unidentified up today. The center of the reefs and the

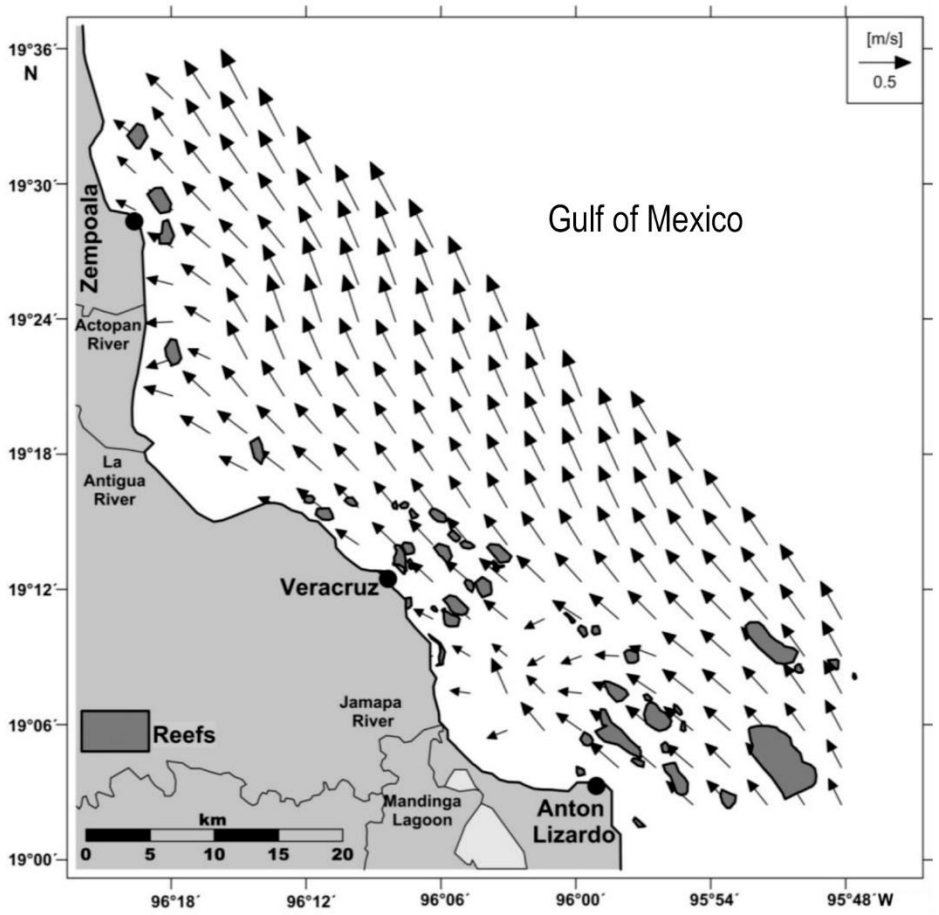

Figure 2. The vertically integrated residual current velocities (m s^{-1}) obtained with the 300-kHz ADCP.

total area of each of the 50 emergent (25 reefs) and submerged (25 reefs) reefs was calculated (Table 1). The limit of each reef was obtained according to their isobaths, using a 15° angle; this was possible since most coral reef structures are located in relatively flat bottom areas. Finally, a visual inspection of the borders was performed in order to avoid any underestimation of the total coral reef area.

RESULTS

The total area of each reef was depicted in Table 1. The total coral reef area of the VRS was calculated in 70.1557 km^2 using the ~1 m resolution bathymetry. The total submerged reef area (7.3446 km^2) was only ~10% of the total area. Not all the submerged reefs were previously identified due to the absence of an accurate bathymetry of the area. It took more than six months to obtain the total bathymetry with a high resolution, which provided an accurate calculation of the total reef area. A total of 48 species were identified, 45 of the order Escleractinia and 3 of the order Anthoathecatae (Table 2). *Acropora prolifera*, a hybrid, was also identified at the VRS. All species were observed at the emerged and submerged reefs.

The vertically integrated currents (Fig. 2) obtained with the ADCP, showed a convergence area off the Jamapa River due to current rectification induced by the southernmost coral reefs, as previously described by Salas-Monreal *et al.* (2009). The same pattern was depicted where the northern reefs deflected the flow, as observed near the town of Zempoala and Actopan River. However, outside the VRS, the current velocities were parallel to the isobaths (Fig. 1) and the coast. This finding is important since the flow is the principal responsible for the dispersion of planktonic organisms. Those organisms were mainly located around the reefs (Fig. 3), as expected due to the vorticity created at abrupt bathymetric changes (Riveron-Enzastiga *et al.*, 2016). The biovolume contours decreased oceanward, mainly due to the distance from the rivers and reefs. Rivers brings nutrients to coastal areas, while reefs and islands generate turbulence which enhances the resuspension of the rich bottom nutrient.

The subtidal temperature gradient obtained with the ADCP, was of ~2°C (Fig. 4), while the salinity gradient

Table 2. Coral reef species found in the Veracruz Reef System.

Order	Suborder	Family	Species
Escleractinia	Astrocoeniina	Acroporidae	*Acropora cervicornis* (Lamarck, 1816)
			Acropora palmata (Lamarck, 1816)
		Astrocoeniidae	*Madracis auretenra* Locke, Weil & Coates, 2007
			Stephanocoenia intersepta (Lamarck, 1836)
		Pocilloporidae	*Madracis decactis* (Lyman, 1859)
		Pocilloporidae	*Madracis pharensis* (Heller, 1868)
	Caryophylliina	Caryophylliidae	*Phyllangia americana* Milne-Edwards & Haime, 1849
			Colangia immersa Pourtalès, 1871
	Dendrophylliina	Dendrophylliidae	*Tubastraea coccinea* Lesson, 1829
	Faviina	Faviidae	*Manicina areolata* (Linnaeus, 1758)
			Montastraea cavernosa (Linnaeus, 1767)
		Meandrinidae	*Dichocoenia stokesi* Milne-Edwards & Haime, 1848
		Merulinidae	*Orbicella annularis* (Ellis & Solander, 1786)
			Orbicella faveolata (Ellis & Solander, 1786)
			Orbicella franksi (Gregory, 1985)
		Mussidae	*Colpophyllia breviserialis* Milne-Edwards & Haime, 1849
			Colpophyllia natans (Houttuyn, 1772)
			Favia fragum (Esper, 1795)
			Mussa angulosa (Pallas, 1766)
			Mycetophyllia danaana Milne-Edwards & Haime, 1849
			Mycetophyllia ferox Wells, 1973
			Mycetophyllia lamarckiana Milne-Edwards & Haime, 1848
			Pseudodiploria clivosa (Ellis & Solander, 1786)
			Pseudodiploria strigosa (Dana, 1846)
			Scolymia cubensis (Milne-Edwards & Haime, 1849)
			Scolymia lacera (Pallas, 1766)
		Oculinidae	*Oculina diffusa* Lamarck, 1816
			Oculina patagonica (de Angelis, 1908)
			Oculina robusta Pourtalès, 1871
			Oculina valenciennesi Milne-Edwards & Haime, 1850
			Oculina varicosa Le Sueur, 1820
	Fungiina	Agariciidae	*Agaricia agaricites* (Linnaeus, 1758)
			Agaricia fragilis Dana, 1848
			Agaricia grahamae Wells, 1973
			Agaricia humilis Verrill, 1902
			Agaricia lamarcki Milne-Edwards & Haime, 1851
			Helioseris cucullata (Ellis & Solander, 1786)
		Poritidae	*Porites astreoides* Lamarck, 1816
			Porites branneri Rathbun, 1888
			Porites colonensis Zlatarski, 1990
			Porites divaricata Le Sueur, 1820
			Porites furcata Lamarck, 1816
			Porites porites (Pallas, 1766)
		Siderastreidae	*Siderastrea radians* (Pallas, 1766)
			Siderastrea siderea (Ellis & Solander, 1786)
Anthoathecatae	Capitata	Milleporidae	*Millepora alcicornis* Linnaeus, 1758
			Millepora complanata Lamarck, 1816
		Stylasteridae	*Stylaster roseus* (Pallas, 1766)

obtained with a CTD, was of ~2 (Fig. 5). The temperature and salinity values ranged from 27.8 to 29.7°C and from 30.5 to 32.6, respectively. The highest temperature values were observed at the reef crest due to the shallowness of the area and the low velocity of the currents. While the salinity values increased oceanward, this is mainly attributed to the distance from the three rivers located in the area (Actopan, La

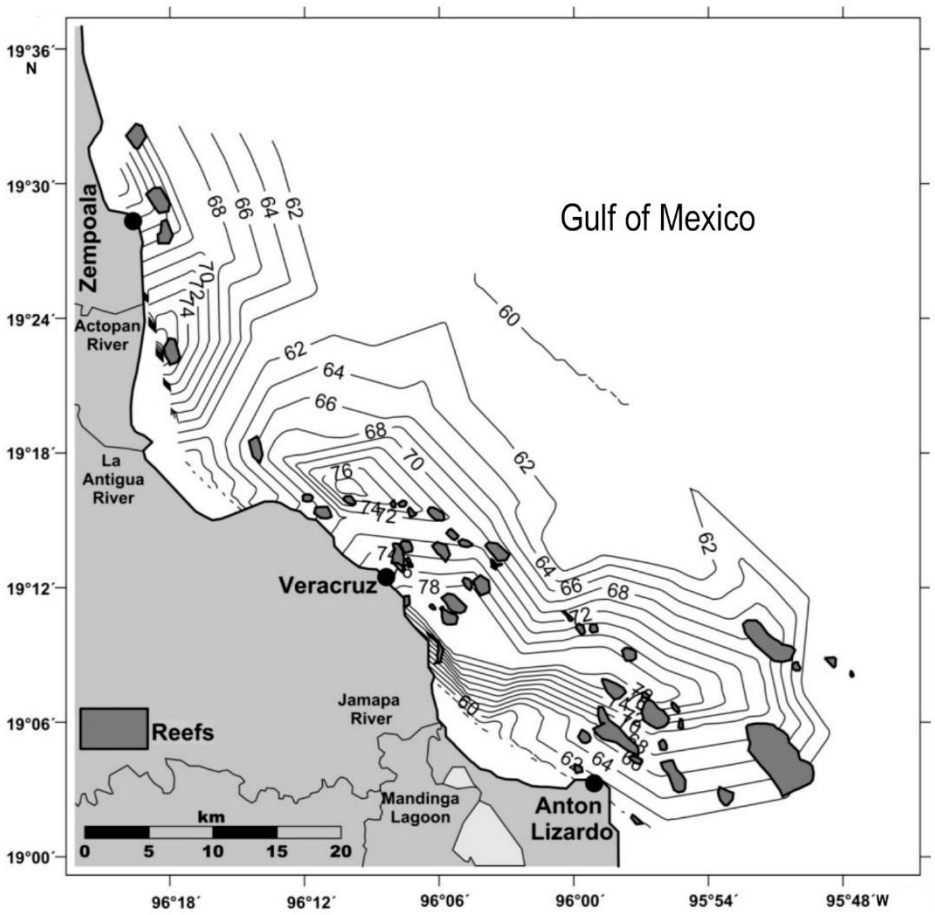

Figure 3. The vertically integrated acoustic scattering volume transformed to biovolumes, obtained with the 300-kHz vessel-mounted ADCP.

Antigua and Jamapa) which brings relatively cold fresh water to the VRS. The halocline (contour maps) obtained with the salinity data, roughly follows the isobaths, leaving most of the reefs with salinity values of ~32.

Finally, the light penetration at 19 m depth (19°10'17"N; 96°05'50"W) near Isla Sacrificios reef (Table 1), suggested a good light bioavailability (Fig. 6). Light intensity values also depicted a similar pattern as the fortnightly tidal signal (M_{sf}). All values ranged from 1,000 to 9,000 lux except for August 9, when an intense rain event was observed. All values below 1,500 lux were also correlated with cloudy days, as for the case of August 5, 27 and 28.

DISCUSSION

A Multibeam sonar combined with the 300-kHz ADCP data were used to obtain the high-resolution bathymetry at the VRS. The ~1 m resolution bathymetry depicted new reef structures, given a total of 50 coral reef structures within the area (Table 1), 27 more than the previously known up today (DOF, 1992). Further, all the northern coral reefs, located off La Antigua and Actopan rivers (Fig. 1) were only locally known or suggested due to current rectification (Salas-Monreal *et al.*, 2017). The coral species and the total area of those reefs were not identified up today. As could be observed in Figure 1, all reefs were located from the coast to a depth of up to 60 m; however when obtaining the percentage of the total coral reef area, most of the area was located between 20 to 40 m depth, this may be one of the reasons why most of the reefs were not previously identified.

A total of 70 species of Scleractinia corals have been identified in the Mexican Caribbean (*e.g.*, Villegas-Sánchez *et al.*, 2013; Horta-Puga *et al.*, 2015), in contrast, only 38 species were previously reported in the VRS (Ortiz-Lozano *et al.*, 2013), in this work we identify 48 species. The higher species richness was recorded in the Los Amarillos and El Rincon reefs with 18 species. There is a reduction in species richness in the submerged reefs located at depths greater than 40 m. One of the most conspicuous species is *Agaricia*

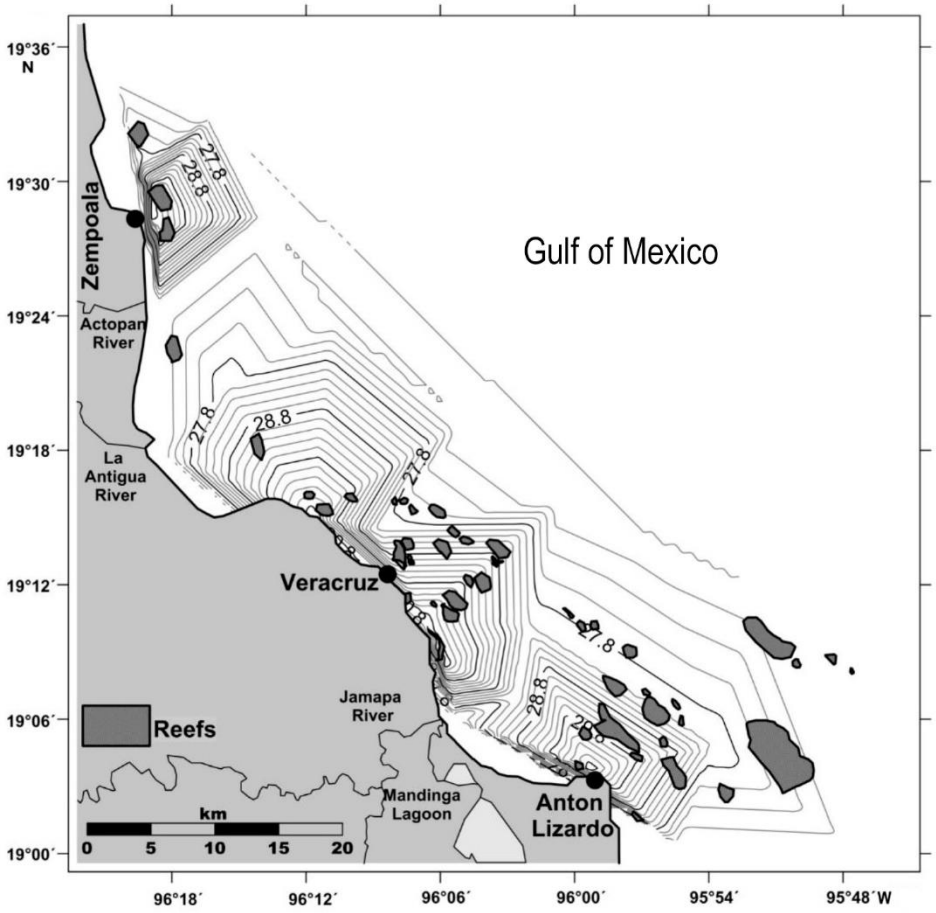

Figure 4. The residual sea surface temperature (°C) obtained with the 300-kHz ADCP.

lamarcki, present and relatively abundant at most reefs. The reduction of the species richness in the submerged reefs is related to light penetration and the concentration of suspended sediments at this depth, which also affects the coral in the clearest waters of the Caribbean Sea (Horta-Puga *et al.*, 2015).

During the summer season, local and mesoscale winds induce a northward current (Riveron-Enzastiga *et al.*, 2016), as could be observed during the sampling period of August 2016. As expected the sea surface temperature and light penetration was higher during clear days than during cloud cover or rain periods. The typically observed flow in coastal areas, parallel to the isobaths (Fig. 2), produced by the cross-coastal geostrophic momentum balance, was also observed here (Salas-Monreal & Valle-Levinson, 2009; Salas-Monreal *et al.*, 2009). However, the diffraction of the coastal currents near the reefs shows the effect of the emerged coral reefs over the typically observed flow (Riveron-Enzastiga *et al.*, 2016). Further, the submerged reefs are responsible for the bottom current rectification, which generates semi-stationary cyclonic gyres as the one previously described by Salas-Monreal *et al.* (2009). The new submerged reefs found at 19°10’48”N, 96°00’00”W (Table 1), combined with the southernmost emerged reefs are the responsible for the current pattern, which concentrates the suspended particles off the Jamapa River. It was previously thought that the Cape of Anton Lizardo was responsible for the pair of cyclonic and anticyclonic gyres observed at this location; however, it was now observed that the presence of submerged reefs at this location generates the gyres. The presence of abrupt bathymetric changes, such as submerged reefs, generates vorticity around them enhancing high productive areas (Riveron-Enzastiga *et al.*, 2016). According to the current patterns (Fig. 2), this should be an area of high concentration of coral larvae during August, which are not reflected in the presence of coral colonies due to the high river discharges during the rainy season (Avendaño-Alvarez *et al.*, 2017). The river discharges in this area induce a moody or sandy bottom, which affects coral settlement. The typically high visibility waters, observed at reef systems, are affected by river

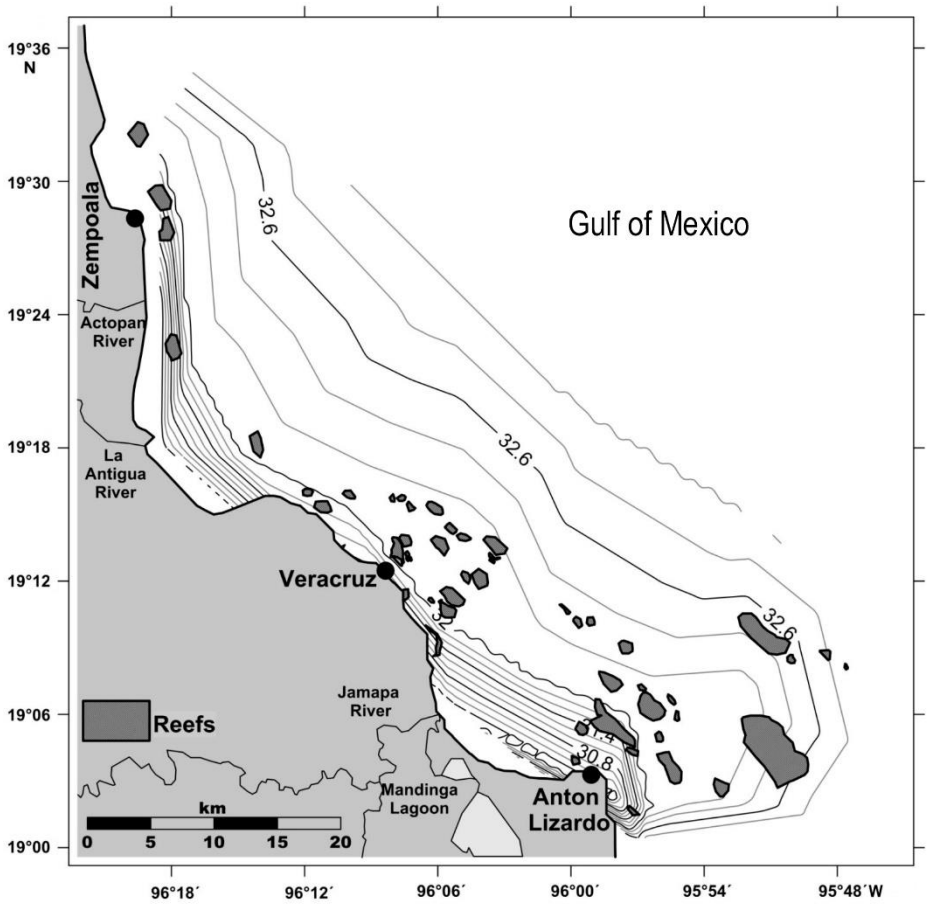

Figure 5. The residual sea surface salinity obtained with a Seabird Term-19.

runoff and gyres, which generated the resuspension of bottom matter (Wolanski & Spagnol, 2000), decreasing light penetration and reducing the depth at which corals may live (Hayward, 1982). The same pattern could be observed off the city of Zempoala and the Actopan River. Areas were coral larvae should concentrate due to current pattern (Fig. 2) but inappropriate for coral settlement due to sandy or moody bottom. This could be confirmed with the biovolumes (Fig. 3), since the convergent areas had concentrations of over 75 dB, while the surrounding waters had values bellow 70 dB, implying that the highest concentration of coral larvae in the northern VRS is located off the city of Zempoala, the Actopan River and near 19°16'48"N, 96°09'01"W. The last location is the only place where coral colonies may develop due to hard bottom, clear water conditions and the convergence of coral larvae coming from the southern reefs, which should be an ideal area for artificial coral reef structures.

The subtidal temperature (Fig. 4) and salinity (Fig. 5) values ranged from 27.8 to 29.7°C and from 30.5 to 32.6, respectively. Those subtidal values are within the optimal values for coral development within the VRS (Avendaño-Alvarez *et al.*, 2017). The isohaline (Fig. 5) is parallel to the isobaths and had a seaward increment from 30.5 to 32.6, with the lowest values near the rivers and off the cities, mainly attributed to the number of cities' drains discharging directly to the VRS. The diurnal tidal variation values, in contrast, may range from 26 to 30°C and from 28 to 32.6, respectively, lower than the previously reported values on August 2006 (Riveron-Enzastiga *et al.*, 2016) and 2012 (Avendaño-Alvarez *et al.*, 2017). The lower values were attributed to a more intense rainy season and higher river discharges during August 2016 when compared to August 2006 and 2012. As expected the highest temperature was found near the reefs and at the shallower areas. While, the lower temperature was found near 19°12'00"N, 96°54'00"W, which correspond to the location of a possible canyon previously described by Riveron-Enzastiga *et al.* (2016). At this location, the canyon generates a bathymetric upwelling, responsible for the lower temperature and relatively high salinity values observed at the surface. It was confirmed with the biovolumes which also showed a

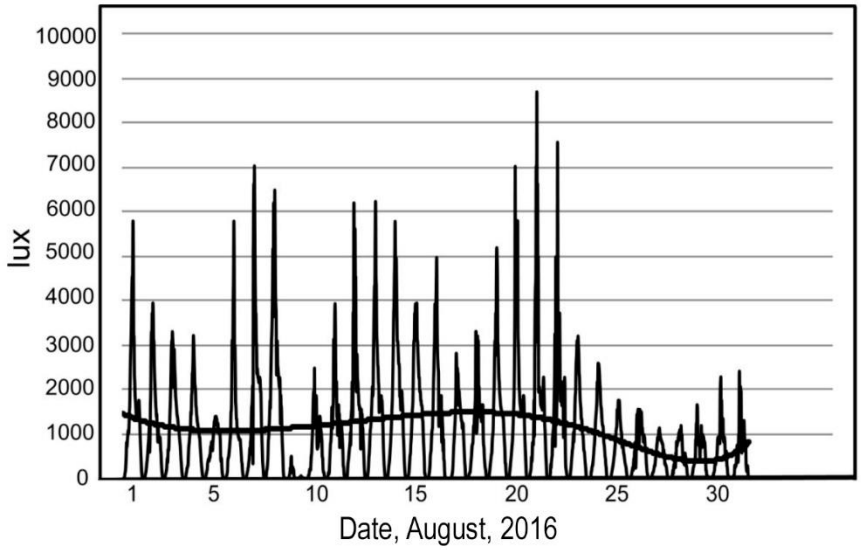

Figure 6. Light intensity (lux) at 19 m depth, near (19°10'17.7816"N; 96°05'50.8452"W) Isla Sacrificios reef obtained with a HOBO (UA-002-64 HOBO).

relatively high concentration value. Even though upwelling regions are characterized by high productive areas (Salas-Monreal *et al.*, 2012), during the spawning period of August, 2016 the zooplankton biovolumes with a size of ~5 mm were higher over the coral reefs (>70 dB) and at the convergent area (>75 dB) than over the topographic upwelling area (>62 dB).

In order to obtain a first approximation of the influence of the river discharges to the VRS, the radio of curvature (r) was then calculated as:

$$r = \frac{U}{f} \quad (1)$$

where U is the surface velocity of the river, averaged at the center of the river mouth from August 27 to 29 (2016) and f is the Coriolis frequency ($f = 2\Omega \sin\Theta$), which is a function of the latitude (Θ). According to (1), and using the river velocity of the Jamapa, La Antigua, and Actopan rivers, as 1.2, 1.3 and 0.8 m s^{-1}, respectively, it was suggested a direct influence of such rivers up to a radius of 32.94, 19.96, and 10.20 km. This is the maximum distance, from the center of the river mouth, at which the salinity, temperature and density values related to river discharges are expected to be found. According to these values, the convergent zone located off the Jamapa River is strongly influenced by sediment transport and salinity fluctuations, making this area inappropriate for coral settlement and development.

Finally, the light penetration at 19 m depth (19°10'17"N; 96°05'50"W) near Isla Sacrificios reef (Table 1), suggested a good light bioavailability (Fig. 6). Light penetration depends on cloud coverage and rain periods. During the last days of August 2016, strong cloud coverage and a four days rain period reduced light penetration at this depth. The light penetration could also be affected by tidal characteristics, the obtained trend (solid black line in Fig. 6) for August (2016) suggested a fortnightly variability, as also observed in tidal sea levels (Salas-Pérez *et al.*, 2012). The fortnightly tidal component (14.79 days) reduces light penetration due to suspended material, mainly brought from the rivers and city drains. Light penetration on August (2016) suggested that even during cloud coverage or rain periods, there was a good light bioavailability for coral colonies at a depth of ~19 m and perhaps during clear days, light bioavailability should reach the bottom everywhere within the VRS (<60 m). This was a case observed during year 2016, since the wet season (rain period) lagged, it does not represent the general behavior of the VRS since the presence of the Jamapa, La Antigua and Actopan rivers must decrease light bioavailability in an average year, perhaps limiting light bioavailability to lower depths (~40 m).

CONCLUSIONS

Current velocities, biovolumes, temperature, salinity, and light intensity time series were obtained at the Veracruz Reef System (VRS), during the coral spawning period of August 2016, to better understand local dynamics and coral larvae dispersion within the VRS. Four concentration areas of coral larvae were identified using the current patterns and the biovolumes; most of those areas are inappropriate for coral settlement and development due to river influence.

During the spawning period of August 2016, the biovolumes at the four convergent areas were higher than the values reported over the rich nutrient bathymetric upwelling area. In order to corroborate the effect of the submerged reefs on current rectification, a new bathymetry was obtained with a high resolution. The ~1 m resolution bathymetry depicted the presence of 50 coral reefs, 27 more than actually known. The total area of the reefs was calculated in 70.1557 km^2. Only ~10% of the total area corresponds to submerged reefs. A total of 48 coral species were identified at the VRS using the new bathymetry, seven more than actually known.

ACKNOWLEDGMENT

The authors would like to acknowledge the effort and dedication of all members of ARGO Consultores, CONANP-Veracruz and the students of the Universidad Veracruzana during the different stages of this work. To the "Administración Portuaria Integral de Veracruz" and the "Comisión Nacional de Áreas Naturales Protegidas de Veracruz" for data availability.

REFERENCES

Avendaño-Alvarez, O., Salas-Monreal, D., Marín-Hernández, M., Salas-de-León, D.A. & Monreal-Gómez, M.A. 2017. Annual hydrological variation and hypoxic zone in a tropical coral reef system. Regional Studies in Marine Science, 9: 145-155.

Alvarado, J.J. & Aguilar, J.F 2009. Batimetría, salinidad, temperatura y oxígeno disuelto en aguas del Parque Nacional Marino Ballena, Pacífico, Costa Rica. Revista de Biología Tropical, 57: 19-29.

Bakun, A. 1996. Patterns in the ocean: ocean processes and marine population dynamics. California Sea Grant, in cooperation with Centro de Investigaciones Biológicas del Noroeste, La Paz.

Biggs, D.C. 1992. Nutrients, plankton, and productivity in a warm-core ring in the western Gulf of Mexico. Journal of Geophysical Research, 97: 2143-2154.

Chacón-Gómez, I.C., Salas-Monreal, D. & Riverón-Enzástiga, M.L. 2013. Current pattern and coral larval dispersion in a tropical coral reef system. Continental Shelf Research, 68: 23-32.

De-la-Lanza-Espino, G. 2001. Características físico-químicas de los mares de México. In: Otero, A. & Pavón, M. (Eds.). Temas selectos de geografía de México. Plaza y Valdés editores, México D.F.

Diario Oficial de la Federación (DOF). 1992. Decreto por el que se declara Área Natural Protegida con carácter de Parque Nacional la zona conocida como Sistema Arrecifal Veracruzano, 24 de agosto de 1992, México.

Farrell, T.M., Bracher, D. & Roughgarden, J. 1991. Cross-shelf transport causes recruitment to intertidal populations in central California. Limnology and Oceanography, 36: 279-288.

Flagg, C.N. & Smith S.L. 1989. On the use of the acoustic Doppler current profiler to measure zooplankton abundance. Deep-Sea Research, 36(3): 455-474.

Hayward, A.B. 1982. Coral reefs in a clastic sedimentary environment: fossil (Miocene, SW Turkey) and modern (Recent, Red Sea) analogues. Coral Reefs, 1(2): 109-114.

Hamner, W.M. & Hauri, I.R. 1981. Effects of island mass: water flow and plankton pattern around a reef in the Great Barrier Reef lagoon, Australia. Limnology and Oceanography, 26(6): 1084-1102.

Holliday, D.V. & Pieper, R.E. 1980.Volume scattering strength sand zooplankton distributions at acoustic frequencies between 0.5 and 3 MHz. Journal Acoustic Society of America, 67(1): 135-146.

Horta-Puga, G., Tello-Musi, J.L., Beltrán-Torres, A., Carricart-Ganivet, J.P., Carriquiry, J.D. & Villaescusa-Celaya, J. 2015. Veracruz Reef System: a hermatypic coral community thriving in a sedimentary terrigenous environment. In: Granados-Barba, A., Ortiz-Lozano, L., Salas-Monreal, D. & González-Gándara, C. (Eds.). Aportes al conocimiento del Sistema Arrecifal Veracruzano: hacia el corredor arrecifal del suroeste del Golfo de México. Universidad Autónoma de Campeche, San Francisco de Campeche, pp. 181-208.

Lalli, C. & Parsons, T.R. 1997. Biological oceanography: an introduction. Butterworth-Heinemann, Oxford.

Lozano-Aburto, M.A. 2008. Toxocenosis de octocorales del Parque Nacional Sistema Arrecifal Veracruzano. Masters Thesis, Universidad Veracruzana, Veracruz, 91 pp.

Mann, K.H., & Lazier, J.R.N. 1991. Dynamics of marine ecosystems. Blackwell Scientific Oxford, 466 pp.

Monreal-Gómez, M.A., Salas-de-León, D.A. & Velasco-Mendoza, H. 2004. La hidrodinámica del Golfo de México. In: Caso, M., Pisanty, I. & Ezcurra, E. (Eds.). Diagnóstico ambiental del Golfo de México, Vol. 1. INE-SEMARNAT, México D.F., pp. 47-68.

Ortiz-Lozano, L., Pérez-España, H., Granados-Barba, A., González-Gándara, C., Gutiérrez-Velázquez, A. & Martos, J. 2013. The reef Corridor of the southwest Gulf of Mexico: challenges for its management and conservation. Ocean and Coastal Management, 86: 22-32.

Riveron-Enzastiga, M.L., Carbajal, N. & Salas-Monreal, D. 2016. Tropical coral reef system hydrodynamics in the western Gulf of Mexico. Scientia Marina, 80(2): 237-246.

Rogers, C.S., Garrison, G., Grober, R., Hillis, Z.M. & Franke, M.A. 2001. Manual para el monitoreo de arrecifes de coral en el Caribe y el Atlántico occidental. Servicio de Parques Nacionales. TNC y WWF, Islas Vírgenes.

Salas-de-León, D.A., Monreal-Gómez, M.A., Signoret, M. & Aldeco, J. 2004. Anticyclonic–cyclonic eddies and their impact on near-surface chlorophyll stocks and oxygen supersaturation over the Campeche Canyon, Gulf of Mexico. Journal of Geophysical Research, 109: C05012.

Salas-Monreal, D. & Valle-Levinson, A. 2009. Sea-level slopes and volume fluxes produced by atmospheric forcing in estuaries: Chesapeake Bay case study. Journal of Coastal Research, 24(2B): 208-217.

Salas-Monreal, D., Salas-de-León, D.A., Monreal-Gómez, M.A. & Riveron-Enzastiga, M.L. 2009. Current rectification in a tropical coral reef system. Coral Reefs, 28(4): 871-879.

Salas-Monreal, D., Salas-de-León, D.A., Monreal-Gómez, M.A., Riveron-Enzastiga, M.L. & Mojica-Ramírez, E. 2012. Hydraulic jump in the Gulf of California. Open Journal of Marine Science, 2(4): 141-155.

Salas-Monreal, D., Salas-Pérez, J.J., Salas-de-León, D.A., Monreal-Gómez, M.A., Pérez-España, H., Ortiz-Lozano, L.D., Granados-Barba, A., Riveron-Enzastiga, M.L. & Villegas-Sánchez, C.A. 2017. Corrientes superficiales dentro del corredor arrecifal del suroeste del Golfo de México. UVserva, 3: 30-35.

Salas-Pérez, J.J. & Granados-Barba, A. 2008. Oceanographic characterization of the Veracruz Reef System. Atmósfera, 21: 281-301.

Salas-Pérez, J.J. & Arenas-Fuentes, V. 2011. Winter water mass of the Veracruz Reef System. Atmósfera, 24(2): 221-231.

Received: 4 May 2018; Accepted: 5 November 2018.

Salas-Pérez, J.J., Salas-Monreal, D., Monreal-Gómez, M.A., Riveron-Enzastiga, M.L. & Llasat, C. 2012. Seasonal absolute acoustic intensity, atmospheric forcing and currents in a tropical coral reef system. Estuarine Coastal and Shelf Science, 100: 102-112.

Storlazzi, C.D., McManus, M.A., Logan, J.B. & McLaughlin, B.E. 2006. Cross-shore velocity shear, eddies, and heterogeneity in water column properties over fringing coral reefs: west Maui, Hawaii. Continental Shelf Research, 26: 401-421.

Trump, C.L. & Marmorino, G. 1997. Calibrating a gyrocompass using ADCP and DGPS data. Journal Atmosphere and Oceanic Technology, 14: 211-214.

Vidal, V.M., Vidal, F.V., Hernández, A.F., Meza, E. & Zambrano, L. 1994. Winter water mass distributions in the western Gulf of Mexico affected by a colliding anticyclonic ring. Journal of Oceanography, 50(5): 559-588.

Villegas-Sánchez, C.A., Pérez-España, H., Rivera-Madrid, R., Salas-Monreal, D. & Arias-González, R.E. 2013. Subtle genetic connectivity between Mexican Caribbean and south-western Gulf of Mexico reefs: the case of the bicolor damselfish, *Stegastes partitus*. Coral Reefs, 1(1): 13-22.

Wolanski, E. & Spagnol, S. 2000. Sticky waters in the Great Barrier Reef. Estuarine Coastal and Shelf Science, 50: 27-32.

Zhu, X-H., Takasugi, Y., Nagao, M. & Hashimoto, E. 2000. Diurnal cycle of sound scatterers and measurements of turbidity using ADCP in Beppu Bay. Journal of Oceanography, 56(5): 559-565.